Table IV. Selected Bond Angles (deg) for $[\eta^5\text{-}C_5(CH_3)_5]W(S)_2[CH_2SiMe_3]$

S(1)–W–S(2)	107.84 (8)	C(5)–C(6)–C(7)	107.1 (5)
S(1)–W–C(1)	101.1 (2)	C(5)–C(6)–C(11)	125.6 (6)
S(2)–W–C(1)	100.5 (2)	C(7)–C(6)–C(11)	127.3 (6)
C(1)–Si–C(2)	113.4 (4)	W–C(7)–C(12)	125.3 (5)
C(1)–Si–C(3)	108.1 (4)	C(6)–C(7)–C(8)	108.4 (6)
C(1)–Si–C(4)	111.1 (4)	C(6)–C(7)–C(12)	124.8 (6)
C(2)–Si–C(3)	108.7 (5)	C(8)–C(7)–C(12)	126.7 (6)
C(2)–Si–C(4)	108.1 (5)	W–C(8)–C(13)	122.5 (5)
C(3)–Si–C(4)	107.2 (4)	C(7)–C(8)–C(9)	107.7 (6)
W–C(1)–Si	121.8 (3)	C(7)–C(8)–C(13)	124.9 (7)
W–C(5)–C(10)	121.5 (5)	C(9)–C(8)–C(13)	127.4 (7)
C(6)–C(5)–C(9)	107.4 (5)	W–C(9)–C(14)	123.7 (5)
C(6)–C(5)–C(10)	125.9 (6)	C(5)–C(9)–C(8)	109.3 (6)
C(9)–C(5)–C(10)	126.3 (6)	C(5)–C(9)–C(14)	123.7 (6)
W–C(6)–C(11)	123.3 (5)	C(8)–C(9)–C(14)	126.9 (6)

A ψ-scan was used to estimate the maximum and minimum transmission coefficients. An empirical absorption correction (DIFABS[40]) was applied. Calculations were performed on a VAX-station 2000 computer using SDP-Plus software developed by Enraf-Nonius and B. A. Frenz & Associates. Positional parameters, bond distances, and bond angles are given in Tables II–IV. Tables of calculated hydrogen positions, thermal parameters, and structure factor tables are provided in the supplementary material.

$(\eta^5\text{-}C_5Me_5)W(=O)(\eta^2\text{-}S_2)Me$. A 0.11 × 0.28 × 0.32 mm crystal was selected and a data set collected by using Mo Kα radiation. Despite a numerical absorption correction, the relatively low transmission (10–37%) and poor crystal quality of this and other crystals yielded a structure of marginal quality, which established the atomic connectivity. Compound **3** crystallizes in the orthorhombic system with a = 14.878 (3) Å, b = 7.202 (3) Å, c = 12.755 (3) Å, V = 1366.8 Å^3, and Z = 4. Anisotropic refinement of tungsten and sulfur atoms and isotropic refinement of other non-hydrogen atoms converged to the residuals R_1 = 0.058 and R_2 = 0.067 in the space group $Pca2_1$ (No. 29). The structure is similar to that of $(\eta^5\text{-}C_5Me_5)W(=O)(\eta^2\text{-}O_2)CH_2SiMe_3$[24] including the alignment of the S–S bond of the η^2-S_2 with the W–Me bond.

Acknowledgment. We wish to thank the National Science Foundation for support of this work.

Supplementary Material Available: Tables S1–S3, listing complete data collection parameters, anisotropic thermal parameters, and calculated hydrogen atom positions (3 pages); Table S4, listing observed and calculated structure factors (18 pages). Ordering information is given on any current masthead page.

(39) Ibers, J. A.; Hamilton, W. C. *Acta Crystallogr.* **1964**, *17*, 781.
(40) Walker, N.; Stuart, D. *Acta Crystallogr.* **1983**, *A39*, 159.

Contribution from the 3M Corporate Research Laboratories, St. Paul, Minnesota 55144, and Department of Chemistry, Stanford University, Stanford, California 94305

Solid-State Chemistry of Molecular Metal Oxide Clusters. Bis(triphenylphosphine)rhodium(I) Carbonyl Derivatives

A. R. Siedle,*,† W. B. Gleason,† R. A. Newmark,† R. P. Skarjune,† P. A. Lyon,† C. G. Markell,† K. O. Hodgson,‡ and A. L. Roe‡

Received June 7, 1989

Hydronium salts of the Keggin-type $XM_{12}O_{40}$ molecular metal oxide cluster anions $SiW_{12}O_{40}^{4-}$, $SiMo_{12}O_{40}^{4-}$, $PW_{12}O_{40}^{3-}$, $PMo_{12}O_{40}^{3-}$, $PMo_{12}O_{40}^{4-}$, and $PVMo_{11}O_{40}^{4-}$ react with $[(Ph_3P)_3Rh(CO)][HC(SO_2CF_3)_2]$ in CH_3CN–C_2H_5OH to form $[trans\text{-}(Ph_3P)_2Rh(CO)(CH_3CN)]_nXM_{12}O_{40}$. These salts lose CH_3CN on heating to provide $[(Ph_3P)_2Rh(CO)]_nXM_{12}O_{40}$, which may also be obtained directly from $[(Ph_3P)_3Rh(CO)][HC(SO_2CF_3)_2]$ in pure ethanol. These oxometalates have been characterized by IR, NMR, and X-ray absorption spectroscopy and are considered to contain isolated, lattice-stabilized $(Ph_3P)_2Rh(CO)(CH_3CN)^+$ and $(Ph_3P)_2Rh(CO)^+$ cations, with the latter being a three-coordinate, 14-electron Rh(I) species. The activity and selectivity of these compounds as catalysts for olefin isomerization and hydroformylation are described. Reaction of $[(Ph_3P)_3Rh(CO)][HC(SO_2CF_3)_2]$ with CH_3CN produces $[trans\text{-}(Ph_3P)_2Rh(CO)(CH_3CN)][HC(SO_2CF_3)_2]$, triclinic, $P\bar{1}$, a = 10.669 (1) Å, b = 22.241 (2) Å, c = 9.257 (5) Å, α = 96.22 (2)°, β = 97.51 (2)°, γ = 79.19 (1)°, Z = 2, V = 2131 Å^3, R = 0.032, and R_w = 0.039.

Introduction

We are seeking to explore and develop the synthetic and solid-state reaction chemistry of organometallic derivatives of molecular metal oxide clusters.[1-3] Clusters of particular interest and utility are the $X^{n+}M_{12}O_{40}^{(8-n)-}$ Keggin ions, where M is molybdenum or tungsten and where the heteroatom X, phosphorus or silicon, has the formal oxidation number n. Examples are $PMo_{12}O_{40}^{3-}$ and $SiW_{12}O_{40}^{4-}$. These anionic clusters have net T_d symmetry and feature a tetrahedral XO_4 unit, at each vertex of which are three edge-shared MO_6 octahedra. The four M_3O_{13} trimeric groups are bonded to one another by corner sharing of oxygen atoms.[4] The $XM_{12}O_{40}^{n-}$ ions are close-packed in the sense that the exterior comprises a cuboctahedral array of oxygen atoms and it is not possible to insert an additional metal atom into the cluster. These features distinguish Keggin ions from lacunary metal oxide clusters: non-close-packed species such as $SiW_{11}O_{39}^{8-}$,[5] A-$PW_9O_{34}^{9-}$,[6] $P_2W_{15}O_{56}^{2-}$,[7] and $P_3O_9^{3-}$[8] into which transition metals may be inserted.

Charge in the $XM_{12}O_{40}^{n-}$ anions is delocalized so that the oxygen atoms lying on the surface of the cluster are weakly nucleophilic. In homogeneous solution, reagents such as R_3O^+ salts are required to effect O-alkylation of $PMo_{12}O_{40}^{3-}$,[9] but heating solid ArN_2^+ salts of $XM_{12}O_{40}^{n-}$ produces $(aryl)_nXM_{12}O_{40}$.[10] Nucleophilicity of anionic molecular metal oxide clusters is substantially increased by using smaller clusters that have a higher charge:mass ratio or by incorporation of group Vb elements.

† 3M Corporate Research Laboratories.
‡ Stanford University.

(1) Siedle, A. R.; Markell, C. G.; Lyon, P. A.; Hodgson, K. O.; Roe, A. L. *Inorg. Chem.* **1987**, *26*, 219.
(2) Siedle, A. R.; Newmark, R. A.; Gleason, W. B.; Skarjune, R. P.; Hodgson, K. O.; Roe, A. L.; Day, V. W. *Solid State Ionics* **1988**, *26*, 1988.
(3) Siedle, A. R. U.S. Pat. 4,673,753.
(4) Pope, M. T. *Heteropoly and Isopoly Oxometallates*; Springer Verlag: New York, 1983.
(5) (a) Knoth, W. H. *J. Am. Chem. Soc.* **1979**, *101*, 2211. (b) Ho, R. K. C.; Klemperer, W. G. *J. Am. Chem. Soc.* **1978**, *100*, 1006.
(6) Knoth, W. H.; Domaille, P. J.; Harlow, R. L. *Inorg. Chem.* **1986**, *25*, 1577.
(7) Finke, R. G.; Droge, M. W. *Inorg. Chem.* **1983**, *22*, 1006.
(8) Besecker, C. J.; Day, V. W.; Klemperer, W. G. *Organometallics* **1985**, *4*, 564.
(9) Knoth, W. H.; Harlow, R. L. *J. Am. Chem. Soc.* **1981**, *103*, 4625.
(10) Siedle, A. R.; Lyon, P. A.; Hunt, S. L.; Skarjune, R. P. *J. Am. Chem. Soc.* **1986**, *108*, 6430.

0020-1669/90/1329-1667$02.50/0

Table I. Analytical and Infrared Data

compd	% calc (% found) C	H	N	P	Rh	ν_{CO}, cm^{-1}
$[(Ph_3P)_2Rh(CO)(CH_3CN)][HC(SO_2CF_3)_2]$ (**1**)	51.7 (51.9)	3.5 (3.5)	1.4 (1.4)			
$[(Ph_3P)_2Rh(CO)(CH_3CN)]_4SiW_{12}O_{40}$ (**2**)	33.1 (33.0)	2.3 (2.2)	1.0 (1.1)	4.4 (4.5)	7.3 (7.0)	2009
$[(Ph_3P)_2Rh(CO)(CH_3CN)]_3PW_{12}O_{40}$ (**3**)	28.2 (28.0)	2.0 (1.9)	0.8 (0.7)			2019
$[(Ph_3P)_2Rh(CO)(CH_3CN)]_3PMo_{12}O_{40}$ (**4**)	35.8 (35.3)	2.5 (2.5)	1.3 (1.0)			2018
$[(Ph_3P)_2Rh(CO)(CH_3CN)]_4SiMo_{12}O_{40}$ (**5**)	40.7 (39.8)	2.9 (2.7)	1.2 (1.2)	5.4 (5.6)	8.9 (8.7)	2008
$[(Ph_3P)_2Rh(CO)]_4SiW_{12}O_{40}$ (**6**)	32.3 (32.9)	2.2 (2.1)	0.0 (<0.1)	4.5 (4.6)	7.5 (7.4)	1990
$[(Ph_3P)_2Rh(CO)]_3PW_{12}O_{40}$ (**7**)	27.7 (28.0)	1.9 (2.1)	0.0 (<0.1)	4.5 (4.7)	6.4 (6.2)	2003
$[(Ph_3P)_2Rh(CO)]_3PMo_{12}O_{40}$ (**8**)	35.2 (35.9)	2.4 (2.7)	0.0 (<0.1)	5.7 (6.0)	8.2 (7.9)	1994
$[(Ph_3P)_2Rh(CO)]_4SiMo_{12}O_{40}$ (**9**)	40.0 (39.8)	2.7 (2.8)	0.0 (<0.1)	5.6 (5.6)	9.3 (9.0)	1993
$[(Ph_3P)_2Rh(CO)]_4PVMo_{11}O_{40}$ (**10**)	40.4 (39.3)	2.7 (2.7)	0.0 (<0.1)	6.3 (6.4)	9.4 (9.6)	1992
$[(Ph_3P)_2Rh(CO)]_4PMo_{12}O_{40}$ (**11**)	40.0 (39.6)	2.7 (2.6)	0.0 (<0.1)			1999

Clusters having organometallic groups covalently bonded to exterior oxygen atoms, e.g. $(CO)_3Mn(Nb_2W_4O_{19})^{3-}$,[11] $[(C_7H_8)Rh]_5(Nb_2O_{19})^{3-}$,[12] $Cp_3Th(NbW_5O_{19})_2^{5-}$,[13] $(Cp_2U)_2(TiW_5O_{19})_2^{4-}$,[14] and $(CpTi)SiV_3W_9O_{40}^{4-}$,[15] have been the objects of a considerable body of innovative synthetic and crystallographic chemistry.[16] The gravamen of this paper is that the $XM_{12}O_{40}^{n-}$ Keggin ions are so weakly nucleophilic that they resist attack by phosphine-substituted Rh(I) cations and that, as a result, coordinatively unsaturated, highly reactive organometallic cations, exemplified by $(Ph_3P)_2Rh(CO)^+$, may be stabilized in the solid state by the lattices provided by the negatively charged molecular metal oxide clusters. A corollary is that such cations are unlikely, except in molten salts or highly acidic fluids,[17] to be readily accessible in homogeneous solution because solvents sufficiently polar to effect ion-pair separation are sufficiently nucleophilic to coordinate the cations.

Synthetic Chemistry

The general synthetic strategy employed in synthesis of transition-metal polyoxometalates proceeds in two steps. The first involves preparation by simple metathetic reactions, carried out in organic solvents, of Keggin ion salts having in the organometallic cation a potentially labile protective or blocking group on the transition-metal site. The protective group is then removed in the second step. This protective group can be an unsaturated hydrocarbyl moiety, such as allyl or cyclooctadiene, that can readily be removed in a solid–gas reaction with hydrogen. Alternatively, it may be a weakly bound ligand such as dinitrogen, which can be removed thermally or photochemically,[10] or acetonitrile, which can be removed simply by heating under vacuum. This second approach has been adapted here to the synthesis of phosphine-substituted Rh(I) derivatives of Keggin ions. Importantly, removal of the protective group, the step that opens a coordination site on the transition metal, is a heterogeneous reaction, carried out in the solid state. In this way, complications due to extraneous solvents, which might serve as potential ligands, are avoided. The only potential ligands or donor sites in such solid-state reaction systems are the oxygen atoms on the exterior of the oxometalate cluster. Ortho-metalation is excluded on the basis of ^{31}P NMR data (vide infra). Demonstration of the presence or absence of chemically significant interactions between the transition-metal-containing cation and these oxygen atoms without resort to X-ray crystallography is very difficult, and we have used extended X-ray absorption fine structure (EXAFS) spectroscopy for this purpose. Because materials containing coordinatively unsaturated organometallic cations are produced in reactions involving solid–solid-phase transformations, it is difficult if not impossible to obtain them as good single crystals even though, in some cases, their precursors crystallize well. Attempts to grow crystals from solution fail because solvents sufficiently polar to dissolve the solid irreversibly coordinate to the organometallic cation.

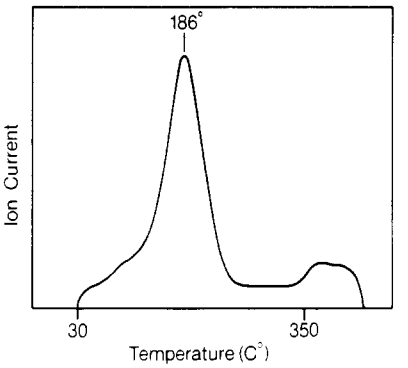

Figure 1. Thermal programmed desorption mass spectrum of $[(Ph_3P)_2Rh(CO)(CH_3CN)]_3PW_{12}O_{40}$ showing m/e 41 (CH_3CN^+) ion current as a function of temperature.

The triphenylphosphine ligand trans to CO in $[(Ph_3P)_3Rh(CO)][HC(SO_2CF_3)_2]$[18,19] is labile, presumably as a result of the trans effect of the carbonyl moiety, and when this salt is treated with acetonitrile, $[trans\text{-}(Ph_3P)_2Rh(CO)(CH_3CN)][HC(SO_2CF_3)_2]$ (**1**) is formed. In situ formation of $(Ph_3P)_2Rh(CO)(CH_3CN)^+$ is a key to synthesis of solids containing the $(Ph_3P)_2Rh(CO)^+$ ion. In addition, the crystal structure of **1**, determined by X-ray crystallography (vide infra), is important in characterization of rhodium oxometalates by X-ray absorption spectroscopy.

Addition of 1 mol of hydrated $(H_3O)_4SiW_{12}O_{40}$ in 3:1 (v/v) ethanol–acetonitrile to 4 equiv of $[(Ph_3P)_3Rh(CO)][HC(SO_2CF_3)_2]$ in the same solvent mixture leads to precipitation in essentially quantitative yield of $[(Ph_3P)_2Rh(CO)(CH_3CN)]_4SiW_{12}O_{40}$ (**2**) as a light yellow, poorly crystalline powder: ν_{CO} 2009 cm^{-1}; ^{31}P MAS δ 27.0 (s) (27.4 ppm, d, J_{RhP} = 120 Hz in propylene carbonate). Similar metathetic reactions were used to prepare $[(Ph_3P)_2Rh(CO)(CH_3CN)]_3PW_{12}O_{40}$ (**3**), $[(Ph_3P)_2Rh(CO)(CH_3CN)]_3PMo_{12}O_{40}$ (**4**), and $[(Ph_3P)_2Rh(CO)(CH_3CN)]_4SiMo_{12}O_{40}$ (**5**). Spectroscopic data, collected in Table I, are all consistent with the formulation of these compounds as Keggin ion salts of $(Ph_3P)_2Rh(CO)(CH_3CN)^+$.

Quantitative loss of acetonitrile from **2**–**5** occurs upon heating. This may be ascertained from elemental analyses and from thermogravimetric analyses. For example, on the heating of **2** under a stream of flowing nitrogen, a 2.6% weight loss (calculated 2.9%) is observed. Thermal programmed desorption (TPD) spectroscopy provides information useful for preparative studies. In this technique, the sample is rapidly heated in the solid inlet probe of a mass spectrometer and the ion currents due to the various volatile species are plotted as a function of temperature. Because T_{max}, the temperature at which evolution of a volatile

(11) Besecker, C. J.; Klemperer, W. G. *J. Am. Chem. Soc.* **1980**, *102*, 7598.
(12) Besecker, C. J.; Klemperer, W. G.; Day, V. W. *J. Am. Chem. Soc.* **1982**, *104*, 6158.
(13) Day, V. W.; Klemperer, W. G.; Maltbie, D. J. *Organometallics* **1985**, *4*, 104.
(14) Day, V. W.; Earley, C. W.; Klemperer, W. G.; Maltbie, D. J. *J. Am. Chem. Soc.* **1985**, *107*, 8261.
(15) Finke, R. G.; Rapko, B.; Domaille, P. J. *Organometallics* **1986**, *5*, 175.
(16) Day, V. W.; Klemperer, W. G. *Science* **1985**, *228*, 533.
(17) Nitschke, J.; Schmidt, S. P.; Trogler, W. C. *Inorg. Chem.* **1985**, *24*, 1972.
(18) (a) Siedle, A. R.; Newmark, R. A.; Pignolet, L. H.; Howells, R. D. *J. Am. Chem. Soc.* **1984**, *106*, 1510. (b) Siedle, A. R.; Newmark, R. A.; Howells, R. D. *Inorg. Chem.* **1988**, *27*, 2473.
(19) Siedle, A. R.; Howells, R. D. U.S. Pat. 4,625,069.

Table II. Thermal Programmed Mass Desorption Spectral Data

compd	$T_{max}(CH_3CN)$, °C	compd	$T_{max}(CH_3CN)$, °C
2	140	**4**	210
3	186	**5**	175

desorbed species peaks, scales, in a first-order process, with the bond dissociation energy,[20] it conveys information about temperatures useful in processing larger, bulk samples. Figure 1 shows the ion current for CH_3CN, m/e 41, between 30 and 400 °C as **3** is heated. There is a well-defined maximum at 186 °C. Accordingly, in preparative-scale reactions, thermal desolvation is effected by heating under vacuum at 190 °C. TPD experiments also show that at higher temperatures, >270 °C, CO and biphenyl are evolved. These presumably arise from decomposition of $(Ph_3P)_2Rh(CO)^+$ and Ph_3P and, in any event, establish upper temperature limits for the pyrolysis reactions. TPD data are given in Table II.

$[(Ph_3P)_2Rh(CO)]_4SiW_{12}O_{40}$ (**6**), synthesized by vacuum pyrolysis of **2** at 150 °C, is a poorly crystalline (by X-ray powder diffraction criteria), pale yellow powder. The CO stretching frequency, 1990 cm^{-1}, is slightly lower than in its solvated precursor. The ^{31}P MAS NMR spectrum demonstrates a broad singlet at 29 ppm (27.2 ppm in propylene carbonate), indicating that the electronic environment about phosphorus is little perturbed upon loss of acetonitrile, and in particular, argues against the presence of an otherwise plausible ortho-metalated structure for the cation, for phosphorus thus incorporated into four- and five-membered rings exhibits large (≥30 ppm) upfield and downfield shifts, respectively,[21] whereas here, the shift on loss of acetonitrile is only +2 ppm. Typically, a weak impurity signal at 22.5 ppm is also observed. The infrared spectrum is, save for the Rh–*CO* region, essentially identical with that of the starting material, i.e. a composite of Ph_3P and $[SiW_{12}O_{40}]^{4-}$ bands. These absorptions are strong and dominate the vibrational spectra so that infrared spectroscopy is, in general, not a useful characterization method other than to show that the basic $XM_{12}O_{40}^{n-}$ structure is preserved. Analogous vacuum pyrolysis procedures were used to prepare $[(Ph_3P)_2Rh(CO)]_3PW_{12}O_{40}$ (**7**), $[(Ph_3P)_2Rh(CO)]_3PMo_{12}O_{40}$ (**8**), and $[(Ph_3P)_2Rh(CO)]_4SiMo_{12}O_{40}$ (**9**) from **3**–**5**, respectively.

Both $[(Ph_3P)_2Rh(CO)(CH_3CN)]_4SiW_{12}O_{40}$ and $[(Ph_3P)_2Rh(CO)]_4SiW_{12}O_{40}$ ionize in solution. The conductances of 1×10^{-4} M solutions in dry propylene carbonate are 540 and 570 Ω^{-1} cm^2 mol^{-1}, respectively. Thus, even this weakly coordinating, high dielectric constant solvent effects ion pair separation.

An alternate synthesis of **6** consists of adding ethanolic hydrated $(H_3O)_4SiW_{12}O_{40}$ to a solution of $[(Ph_3P)_3Rh(CO)][HC(SO_2CF_3)_2]$ in hot (70 °C) ethanol under nitrogen. The compound precipitates, is isolated by filtration, and then is dried under high vacuum. Dissociation of the CO and Ph_3P ligands from the $HC(SO_2CF_3)_2^-$ salt of $(Ph_3P)_3Rh(CO)^+$ is not observable by ^{13}C or ^{31}P NMR at room temperature in CH_2Cl_2, but empirically, dissociation of Ph_3P occurs to give $(Ph_3P)_2Rh(CO)^+$, which is intercepted and precipitated by the large silicotungstate anion. Compounds **6**–**9** prepared by this method are identical by elemental, ^{31}P MAS NMR, and infrared analyses with samples obtained by the thermal desolvation route.

Although satisfactory elemental analyses for these rhodium oxometalates have been obtained, cf. Table I, additional compositional characterization data are needed to be sure that these compounds do not contain significant amounts of solvent. Salts of large metal oxide cluster anions frequently separate in forms containing lattice or zeolitic solvent, complete removal of which is difficult. Furthermore, ethanol or water might be coordinated to rhodium in **6**–**9** and the presence of such coordinated solvent would negligibly affect analytical data for such high molecular weight compounds. Solutions of **2**, **3**, **6**, and **7** in scrupulously dry dmso-d_6 were analyzed by ^1H NMR spectroscopy for acetonitrile, ethanol, and water. The results, expressed as moles solvent per mole of rhodium, are given in Table III. In no case are sufficient residual solvents present in amounts sufficient to coordinate all the $(Ph_3P)_2Rh(CO)$ units. For example, **6** (prepared in neat ethanol) contains 0.20 mol of ethanol and 0.02 mol of water/mol of Rh, and we consider that this reflects the presence of residual zeolitic or lattice solvent.

Table III. NMR Analyses for Residual Solvents

	mol of solvent/mol of Rh		
compd	H_2O	C_2H_5OH	CH_3CN
2	0.00	0.10	0.96
3	0.07	0.08	0.97
6[a]	0.20	0.02	0.00
7[a]	0.00	0.30	0.00

[a] Prepared by thermal desolvation, method A.

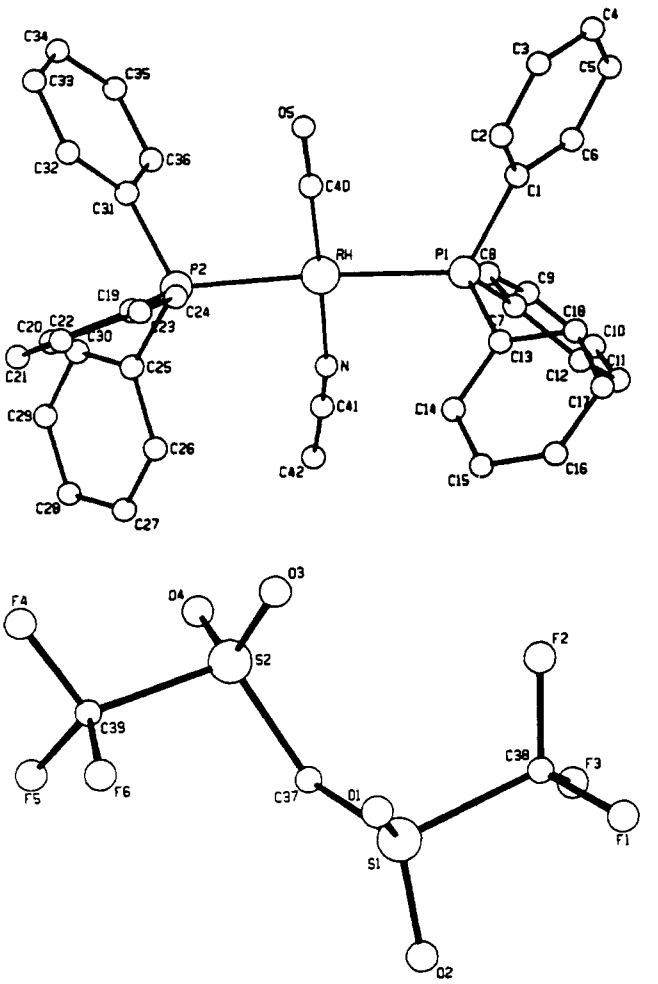

Figure 2. PLUTO drawing of the cation and anion in [*trans*-$(Ph_3P)_2Rh(CO)(CH_3CN)][HC(SO_2CF_3)_2]$.

Desolvation and loss of acetonitrile from **2** is reversible. When $[(Ph_3P)_2Rh(CO)]_4SiW_{12}O_{40}$ is heated with liquid acetonitrile, uptake of 1 mol of the nitrile/mol of rhodium occurs. Nitrogen analysis indicates that **2** has been regenerated. The CO stretching frequency shifts back to 2009 cm^{-1}. In addition, the infrared spectrum then demonstrates weak bands at 2290 and 2325 cm^{-1} (cf. 2360 cm^{-1} for free CH_3CN), which shows that the acetonitrile is coordinated to Rh(I) and that it is not present as a lattice solvate.

Structural Studies

The structure of $[(Ph_3P)_2Rh(CO)(CH_3CN)][HC(SO_2CF_3)_2]$ has been determined in order to provide structural parameters for the rhodium cation. A PLUTO view and labeling scheme are shown in Figure 2. Selected bond distances and angles are given in Table IV. In *trans*-$(Ph_3P)_2Rh(CO)(CH_3CN)^+$, Rh(I) exhibits square-planar coordination geometry, as indicated by the bond

(20) Redhead, P. A. *Trans. Faraday Soc.* **1961**, *57*, 641.
(21) Garrou, P. E. *Chem. Rev.* **1981**, *81*, 229.

Table IV. Selected Bond Distances and Angles in [*trans*-$(Ph_3P)_2Rh(CO)(CH_3CN)][HC(SO_2CF_3)_2]$ (**1**)

	Distances (Å)		
Rh–P1	2.340 (1)	C37–S2	1.652 (4)
Rh–P2	2.336 (1)	S1–O1	1.424 (3)
Rh–C40	1.809 (4)	S1–O2	1.424 (3)
Rh–N	2.048 (3)	S2–O3	1.414 (3)
C40–O5	1.142 (5)	S2–O4	1.429 (3)
N–C41	1.113 (4)	S1–C38	1.812 (6)
C37–S1	1.647 (4)	S2–C39	1.824 (6)
	Angles (deg)		
P1–Rh–C40	92.3 (1)	N–C41–C42	177.8 (5)
P–Rh–N	90.2 (1)	Rh–N–C41	168.0 (3)
P2–Rh–C40	92.3 (1)	S1–C37–S2	125.3 (4)
P2–Rh–N	89.9 (1)	O1–S1–O2	120.0 (2)
		O3–S2–O4	119.8 (2)

angles about the metal and by the deviations from the Rh,P2,P1,C40,N least-squares plane, which are 0.005, 0.121, 0.117, −0.129, and −0.114 Å, respectively. The carbonyl ligand is essentially linear [∠Rh–C40–O5 = 177.2 (4)°], with d(C40–Rh) = 1.809 (4) Å. So too is the CH_3CN ligand, with d(Rh–N) = 2.048 (3) Å and ∠C41–N–Rh = 168.0 (3)°. The geometry of the $HC(SO_2CF_3)_2^-$ anion is that previously found in many organometallic salts, and it exhibits a slight asymmetry in the S–O bond lengths.[22,23]

Rhodium EXAFS spectra have been obtained for [*trans*-$(Ph_3P)_2Rh(CO)(CH_3CN)][HC(SO_2CF_3)_2]$, for which independent structural data are available, $[(Ph_3P)_2Rh(CO)(CH_3CN)]_4SiW_{12}O_{40}$, and $[(Ph_3P)_2Rh(CO)]_4SiW_{12}O_{40}$. X-ray absorption data were collected at −173 °C. Use of low-temperature data minimizes the possibility that thermal vibrations and rotation of the cluster anions could obscure important structural features. The Fourier transforms of the rhodium K-edge spectra of the two rhodium oxometalate compounds are shown in Figure 3a and compared with that of $(Bu_4N)[(Me_5C_5Rh)W_5O_{18}(TiC_5H_5)]$. The transforms of the spectra of **2** and **6** are seen to be quite similar and are dominated by backscattering from the two phosphorus atoms [d(Rh–P) = 2.3 Å] in the first coordination core. No backscattering from tungsten is observed, but it is readily apparent in the transformation of the EXAFS spectrum of $(Bu_4N)[(Me_5C_5Rh)W_5O_{18}(TiC_5H_5)]$. This model compound has been crystallographically characterized, and in it, d(Rh–W) is 3.26 Å.[24] On this basis, we believe that rhodium is not coordinated to the exterior oxygen atoms in the $SiW_{12}O_{40}$ cluster and, therefore, that $[(Ph_3P)_2Rh(CO)]_4SiW_{12}O_{40}$ contains isolated $(Ph_3P)_2Rh(CO)^+$ ions, which are located in interstitial sites in a lattice comprising $SiW_{12}O_{40}^-$ ions. The absorption edges of **2** and **6** (Figure 3b) are essentially congruent. Because both the EXAFS and edge structure are sensitive to significant changes in the coordination environment of the absorbing metal, here Rh, it appears that the electronic features of Rh in both compounds are quite similar. This is the expected result of loss of a weakly bonding ligand such as CH_3CN and is in accord with the rather small changes in ν_{CO} and $\delta(^{31}P)$ upon loss of CH_3CN, which converts **2** to **6**. Only consistent with the presence of effectively isolated $(Ph_3P)_2Rh(CO)^+$ ions in these compounds is the observation that increasing the negative charge on the molecular metal oxide cluster by −1 by replacement of molybdenum by vanadium or by one-electron reduction has little effect on the carbonyl stretching frequency. Thus, ν_{CO} values in $[(Ph_3P)_2Rh(CO)]_4PVMo_{11}O_{40}$ (**10**) and $[(Ph_3P)_2Rh(CO)]_4PMo_{12}O_{40}$ (**11**) are 1992 and 1999 cm^{-1}, respectively.

Catalytic Chemistry

Because of the very high probability of reaction of $[(Ph_3P)_2Rh(CO)]_4SiW_{12}O_{40}$ with solvents in which it is soluble, heterogeneous catalytic chemistry of this and other rhodium oxometalates was explored in reactions in which the catalyst was suspended in toluene. This nonreactive hydrocarbon appears not to dissolve **1** or any of the Keggin ion salts and provides a convenient heat-transfer medium. Complexes of Rh(I) are known to function as catalysts for the olefin rearrangement and hydroformylation, and so these reactions were examined in order to develop structure–reactivity correlations. Compounds **2** and **6** have been studied in greatest detail, but we find that, in general, the catalytic chemistry of other rhodium oxometalates reported here parallels that of these two materials.

Table V. Products from Hydroformylation of 1-Hexene

	yield, %		
catalyst	1-hexene	*n*-hexane	aldehydes
$[(Ph_3P)_3Rh(CO)][HC(SO_2CF_3)_2]$	0.1	0.5	97
2	0.2	10	89
6	0.04	4	95

Table VI. Distribution of C_7 Aldehydes Obtained by Using (Triphenylphosphine)rhodium Carbonyl Oxometalate Hydroformylation Catalysts

		distribution, %		
substrate–catalyst	aldehyde yield, %	heptanal	2-methyl-hexanal	2-ethyl-pentanal
1-hexene–**6**	95	57	36	7
2-hexene–**6**	96	13	57	30
3-hexene–**6**	92	10	40	50
1-hexene–**7**	95	51	39	10
1-hexene–**8**	92	54	38	8
1-hexene–**9**	93	60	34	5
1-hexene–**10**	96	64	33	3

Reaction at 100 °C of 1-hexene with a toluene suspension of **2** or **6** produces a mixture of hexene isomers that, by ^{13}C NMR analysis, is comprised of 59% *trans*-2-hexene, 25% *cis*-2-hexene, 9% *trans*-3-hexene, 2% *cis*-3-hexene, and 5% 1-hexene. This isomerization process, which presumably occurs contemporaneously with olefin hydroformylation (vide infra), accounts for at least some of the formation of branched chain aldehydes from 1-hexene.

Hydroformylation of 1-hexene is catalyzed by **1** and the compounds $[(Ph_3P)_2Rh(CO)(CH_3CN)]_nXM_{12}O_{40}$ and $[(Ph_3P)_2Rh(CO)]_nXM_{12}O_{40}$. The yields of aldehydes produced, and of the hydrogenation product, *n*-hexane, are collected in Table V. These three catalysts exhibit distinct differences in their selectivity for olefin hydroformylation relative to hydrogenation. Of the three materials, $[(Ph_3P)_2Rh(CO)(CH_3CN)]_4SiW_{12}O_{40}$ is least selective and the hexane:aldehyde ratio in the product is 0.12 compared with 0.04 and 0.005 for $[(Ph_3P)_2Rh(CO)]_4SiW_{12}O_{40}$ and $[(Ph_3P)_3Rh(CO)][HC(SO_2CF_3)_2]$, respectively. As stated above, formation of branched aldehydes can be due to prior isomerization of the olefin substrate and/or lack of selectivity in the hydroformylation reaction. That involvement of olefin isomerization is kinetically significant is indicated by the data in Table VI, which shows the distribution of C_7 aldehydes obtained from hydroformylation of 1-, 2-, and 3-hexene using $[(Ph_3P)_2Rh(CO)]_4SiW_{12}O_{40}$ as the catalyst. For example, 2-ethylpentanal, which cannot arise directly from 1-hexene comprises 7.4% of the aldehydes derived from this hydrocarbon. The active sites in hydroformylation chemistry are doubtless the Rh(I) centers; WO_3 and $(n\text{-}Bu_4N)_4SiW_{12}O_{40}$ exhibit no detectable activity as catalysts.

When C_7 aldehydes are allowed to stand in air in the presence of **2** or **6**, the corresponding C_7 carboxylic acids are formed over the course of several weeks. More rapid, preparative-scale oxidations may be carried out in an autoclave at 100 °C under 650 psig of air pressure. Under these conditions, the yields of acids are quantitative, but that using **1** is only 16%, thus indicating that it is the metal oxide cluster portion of **2** or **6** that is active in transferring oxygen to the aldehyde. The distribution of C_7 carboxylic acids always tracks that of the corresponding aldehydes, and therefore aldehyde isomerization does not occur to a significant degree under the above reaction conditions. Sequential hydro-

(22) Siedle, A. R.; Gleason, W. B.; Newmark, R. A.; Pignolet, L. H. *Organometallics* **1986**, *5*, 1969.
(23) The crystal structures of $H_2C(SO_2CF_3)_2$, $HN(SO_2CF_3)_2$, and the $(n\text{-}C_3H_7)_4N^+$ salts of their conjugate bases have been determined and will be reported separately.
(24) Day, V. W.; Klemperer, W. G. Unpublished results.

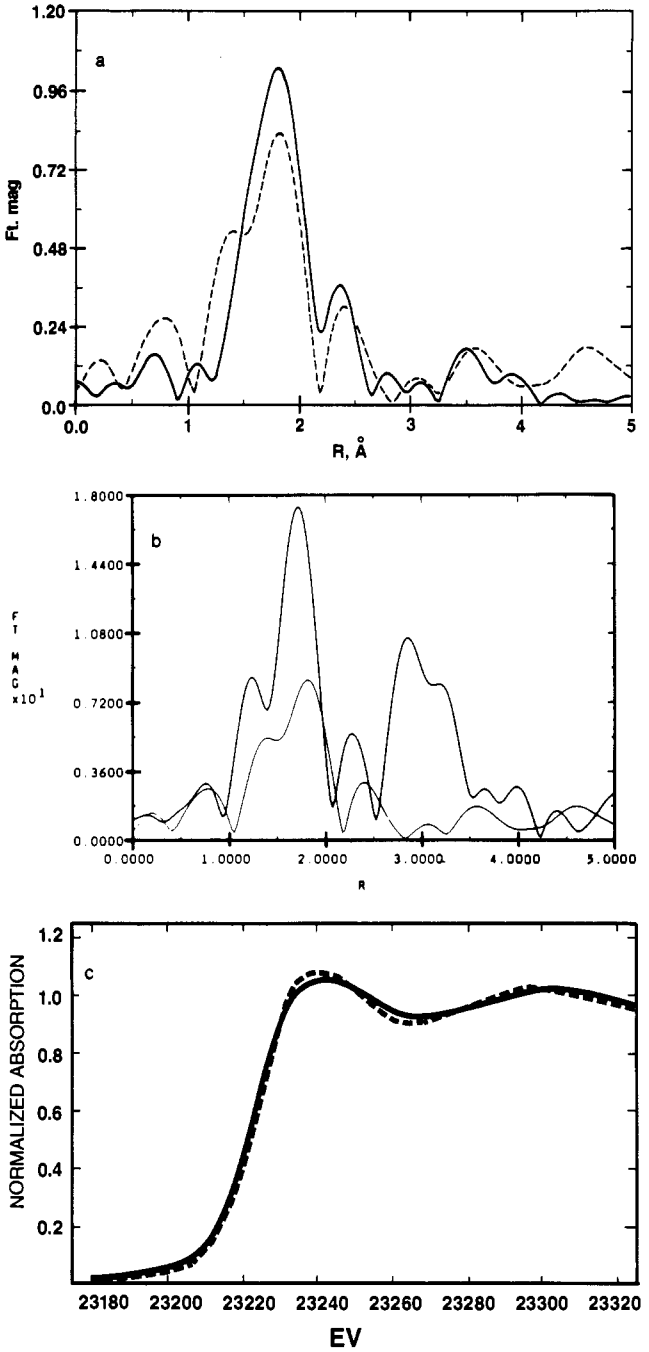

Figure 3. (a) Fourier transform of background-subtracted Rh K-edge EXAFS spectra of $[(Ph_3P)_2Rh(CO)(CH_3CN)]_4SiW_{12}O_{40}$ (**2**) (solid line) and $[(Ph_3P)_2Rh(CO)]_4SiW_{12}O_{40}$ (**6**) (dashed line). (b) Comparison of Fourier transforms of Rh K-edge EXAFS spectra of **6** and $(Bu_4N)_2[(Me_5C_5Rh)W_5O_{18}(TiC_5H_5)]$. (c) Normalized Rh K-edge spectra of **2** (solid line) and **6** (dashed line).

formylation–oxidation of 1,3-butadiene produced a 2:1 mixture of *n*-pentanoic and 2-methylbutanoic acids. Failure to obtain any adipic acid may be attributed to rapid hydrogenation of the intermediate unsaturated aldehyde. Thus, $[(Ph_3P)_2Rh(CO)]_4SiW_{12}O_{40}$ and the related compounds described here are bifunctional catalysts in that they are capable of activating carbon monoxide and hydrogen at the Rh(I) centers and aldehydes at the $SiW_{12}O_{40}$ cluster. The mechanism of aldehyde oxidation has not been established. On the basis of previous work, we suggest that transfer of the C(O)–*H* hydrogen atom to the oxide cluster is involved.[25]

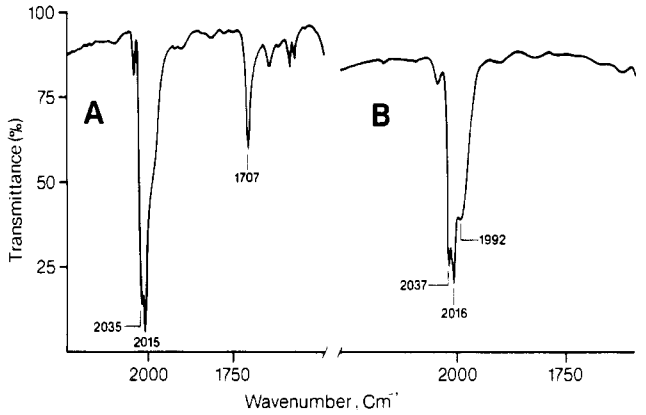

Figure 4. Infrared spectra in the carbonyl stretching region of $[(Ph_3P)_2Rh(CO)]_4SiW_{12}O_{40}$ after exposure to (A) 2000 psig of CO and (B) 200 psig of CO.

In an effort to characterize possible intermediates in the catalytic hydroformylation reactions, solid $[(Ph_3P)_2Rh(CO)]_4SiW_{12}O_{40}$ was treated with 200 psig of carbon monoxide. The infrared spectrum of the product (Figure 4b) shows, in addition to a band due to the starting material, two new absorptions at 2035 and 2016 cm^{-1}. Only these new bands appeared when **6** was treated with 1:1 H_2–CO at 1000 psig. The two new carbonyl bands are attributed to $[(Ph_3P)_2Rh(CO)_3]_4SiW_{12}O_{40}$ (**12**) and agree well with ν_{CO} 2037 and 2016 cm^{-1} reported for $[(Ph_3P)_2Rh(CO)_3][BPh_4]$.[26] On standing in air or under vacuum, **12** loses CO and re-forms **6**. Conversion of **6** to **12** under 200 psig of CO pressure is estimated to be about 50%. When the CO pressure is increased to 2000 psig, conversion is seen from the infrared spectrum (Figure 4a) to be essentially quantitative. However, when this higher pressure of CO is employed, an additional new absorption, at 1707 cm^{-1}, is also observed. It occurs in a frequency range characteristic of Rh–CO–Rh bridging C–O stretching. This datum logically requires that, in the species giving rise to the 1707-cm^{-1} band, two Rh(I) centers be ≤3 Å apart. We consider it to be quite unlikely indeed that any ions having such a short Rh–Rh distance are present in **6** before reaction with CO. Rather, we surmise that, under very high pressures of CO, a high steady state concentration of a mobile phosphine-substituted Rh(I) species is produced that is sufficient to allow formation of a binuclear Rh(I) compound. In other words, under some circumstances, large organometallic cations, encumbered as they are with bulky organophosphine ligands, can move through the open lattices provided by molecular metal oxide clusters and couple. Absent definitive, real-time characterization of **6** under elevated CO pressure, further speculation on the nature of the Rh–CO–Rh species is unwarranted. However, significant cation mobility does occur in $[(Et_3P)_2PtH]_3PW_{12}O_{40}$, leading to formation of a Pt_2 dimer.[27]

The compound $[(Ph_3P)_2Rh(CO)]_4SiW_{12}O_{40}$ is also a heterogeneous catalyst for the oxidation of CO by NO to form carbon dioxide (eq 1), a reaction pathway more commonly found on

$$2NO + 2CO \rightarrow 2CO_2 + N_2 \quad (1)$$

$$2NO + CO \rightarrow CO_2 + N_2O \quad (2)$$

metallic surfaces. Molecular organometallic materials such as $(Ph_3P)_2IrBr(NO)_2$,[28] $[(Ph_3P)_2Rh(NO)_2][PF_6]$,[29,30] ethanolic $RhCl_3 \cdot nH_2O$,[31] and $Rh(CO)_2Cl_2^-$ salts,[32] on the other hand, are homogeneous catalysts for the disproportionation of CO and NO (eq 2).

(25) (a) Hill, C. L.; Bouchard, D. A. *J. Am. Chem. Soc.* **1985**, *107*, 5148. (b) Fox, M. A.; Cardona, R.; Gaillard, E. *J. Am. Chem. Soc.* **1987**, *109*, 6347. (c) Misono, M. *Catal. Rev.—Sci. Eng.* **1987**, *29*, 1987. (d) Highfield, J. G.; Moffat, J. B. *J. Catal.* **1986**, *98*, 245.

(26) Schrock, R. R.; Osborn, *J. Am. Chem. Soc.* **1971**, *93*, 2397.
(27) Siedle, A. R.; Newmark, R. A.; Day, V. W. Manuscript in preparation.
(28) Haymore, B. L.; Ibers, J. A. *J. Am. Chem. Soc.* **1974**, *96*, 3325.
(29) Bhaduri, S.; Johnson, B. F. G. *Transition Met. Chem.* **1978**, *3*, 3325.
(30) Bhaduri, S.; Johnson, B. F. G.; Savory, C. J.; Segal, J. A.; Walter, R. H. *J. Chem. Soc., Chem. Commun.* **1974**, 809.
(31) Reed, J.; Eisenberg, R. *Science* **1974**, *184*, 568.
(32) Hendricksen, D. E.; Neyer, C. D.; Eisenberg, R. *Inorg. Chem.* **1977**, *16*, 970.

Table VII. Crystallographic Data for $[(Ph_3P)_2Rh(CO)(CH_3CN)][HC(SO_2CF_3)_2]$

chem formula $C_{42}H_{34}F_6NO_5P_2RhS_2$	fw 975.71
a = 10.669 (1) Å	space group $P\bar{1}$
b = 22.241 (2) Å	T = 23 °C
c = 9.257 (5) Å	λ = 0.71069 Å
α = 96.22 (2)°	ρ_{calcd} = 1.52 g cm^{-3}
β = 97.51 (2)°	μ = 6.3 cm^{-1}
γ = 79.19 (1)°	max, min, av transm factors:
V = 2131.1 Å^3	0.959, 0.998, 0.982
Z = 2	R = 0.032
	R_w = 0.039

Initial results described here with phosphine-substituted rhodium carbonyl derivatives of Keggin-type molecular metal oxide clusters indicates that these large, anionic globular cages form lattices useful for the stabilization of highly reactive, coordinatively unsaturated organometallic cations.

Experimental Section

Hydrated $(H_3O)^+$ salts of Keggin ions were obtained commercially; that of $PVMo_{11}O_{40}^{4-}$ was prepared by the method of Tsigdinos.[33] The salt $[(Ph_3P)_3Rh(CO)][HC(SO_2CF_3)_2]$ (**1**) was obtained from the reaction of $(Ph_3P)_3Rh(CO)H$ and $H_2C(SO_2CF_3)_2$ in toluene.[19] Infrared spectra were obtained on samples as Nujol mulls; frequency listings are believed to be accurate to ≤5 cm^{-1}. ^{31}P MAS spectra were obtained at 81 MHz with ^{1}H cross-polarization; chemical shifts are expressed relative to external 85% H_3PO_4 as are 162-MHz solution phase data. Proton and carbon-13 NMR spectra were obtained on a Varian XL-400 instrument. Thermal programmed desorption mass spectra were measured as previously described.[34]

GC–MS analyses were performed on a Hewlett-Packard 5995 instrument having a J & W Scientific 30 m × 0.25 mm fused silica DB-5 column and a 1-μm film thickness. Column operating conditions were as follows: temperature 50 °C with a 2-min hold, programmed at 10 °C min^{-1} to 250 °C with a 2-min hold; injector temperature 300 °C; column heat pressure 26 psi of He; split ratio 20:1 with approximately 2 μL of sample diluted to 0.5% in CH_2Cl_2. Routine GC analyses were carried out on a HP 5880 gas chromatograph equipped with a 50 m × 0.32 mm HP SE-54 fused silica having a 1-μm film thickness. Column operating conditions were as follows: temperature 60 °C with a 2-min hold, programmed to 250 °C at 10 °C min^{-1}; FID temperature 250 °C; injector temperature 260 °C; column head pressure 15 psi of He; split ratio 90:1 with 3-μL sample. Retention times of heptanal and heptanoic acid under these conditions were 8.76 and 12.02 min, respectively. Small reference samples of 2-ethylpentanal and 2-ethylpentanoic acid were prepared by oxidation of 2-ethylpentanol (Wiley Chemical Co.) with pyridinium chlorochromate in dimethylformamide. These were purified by preparative gas chromatography.

X-ray absorption coefficients were determined at energies between 22 800 and 23 800 eV and the rhodium EXAFS analyzed by previously described procedures.[35] Measurements were obtained in the transmission mode by using X-radiation from the Stanford Synchrotron Radiation Laboratory, Si(220) monochromators, and argon-filled ionization chambers. Data were collected on beam-line VII-3 at −173 °C by using an Oxford Instruments cryostat and an approximately 0.03-g sample mixed homogeneously with boron nitride.

Routine C and H elemental analyses, when applied to the new oxometalate compounds reported here, only infrequently gave acceptable results. We speculate that this is due to the formation of adamant tungsten carbide. Our carbon analyses were performed by Doris Peters of the 3M Analytical and Properties Research Laboratory using a Leco CS-344 instrument. In it, the sample is mixed with a metallic iron flux and then inductively heated to 2500 °C in a stream of oxygen. Carbon in the analyte is converted to CO_2 that is measured by an infrared detector. For these compounds, we consider that ±1% deviation in carbon content is an acceptable result.

$[(Ph_3P)_2Rh(CO)(CH_3CN)][HC(SO_2CF_3)_2]$ (1). A solution of 0.6 g of $[(Ph_3P)_3Rh(CO)][HC(SO_2CF_3)_2]$ in 3 mL of acetonitrile and 5 mL of toluene was concentrated under reduced pressure until solids appeared and then chilled. Filtration afforded 0.35 g of **1** as yellow crystals, which were used for X-ray diffraction experiments. NMR ($CDCl_3$): ^{31}P, 30.8 (d, J_{RhP} = 119 Hz); ^{1}H, 3.18 [$HC(SO_2CF_3^-)$], 1.14 (CH_3CN). IR (Nujol): ν_{CO} 2010 (s), 1960 (w) cm^{-1}.

$[(Ph_3P)_2Rh(CO)(CH_3CN)]_4SiW_{12}O_{40}$ (2). To a solution of 0.59 g of $[(Ph_3P)_3Rh(CO)]HC(SO_2CF_3)_2$ in 10 mL of 3:1 (v/v) acetonitrile–ethanol was added dropwise with stirring 0.41 g of hydrated $(H_3O)_4SiW_{12}O_{40}$ in 4 mL of the same solvent mixture. The product separated as a gummy precipitate that solidified on vigorous stirring. It was collected on a filter, washed with fresh solvent, and dried at 30 °C under high vacuum. The yield was 0.63 g.

Table VIII. Positional Parameters and Their Estimated Standard Deviations[a]

atom	x	y	z	B, Å^2
Rh	0.99883 (3)	0.24969 (1)	0.26480 (3)	2.835 (6)
S1	0.4330 (1)	0.17838 (5)	−0.3237 (1)	5.12 (3)
S2	0.4964 (1)	0.29033 (6)	−0.1561 (1)	5.54 (3)
P1	0.98999 (9)	0.14936 (4)	0.1630 (1)	2.82 (2)
P2	1.00010 (9)	0.35295 (4)	0.3438 (1)	2.79 (2)
F1	0.2537 (3)	0.1178 (2)	−0.2923 (5)	12.7 (1)
F2	0.2566 (3)	0.1978 (2)	−0.1434 (4)	11.0 (1)
F3	0.3961 (4)	0.1189 (2)	−0.1102 (4)	11.9 (1)
F4	0.5447 (3)	0.3888 (1)	−0.2509 (4)	9.2 (1)
F5	0.6926 (3)	0.3115 (2)	−0.2700 (4)	10.5 (1)
F6	0.5233 (4)	0.3166 (2)	−0.4188 (4)	10.4 (1)
O1	0.3449 (3)	0.2157 (2)	−0.4208 (4)	7.4 (1)
O2	0.5044 (3)	0.1217 (2)	−0.3785 (4)	7.3 (1)
O3	0.3647 (3)	0.3166 (2)	−0.1775 (5)	9.0 (1)
O4	0.5701 (4)	0.3025 (2)	−0.0191 (4)	8.3 (1)
O5	0.7470 (3)	0.2637 (1)	0.3754 (4)	6.99 (8)
N	1.1854 (3)	0.2396 (1)	0.2217 (4)	4.01 (8)
C1	0.8886 (3)	0.1044 (2)	0.2353 (4)	2.98 (8)
C2	0.7566 (4)	0.1255 (2)	0.2273 (5)	4.3 (1)
C3	0.6794 (4)	0.0931 (2)	0.2841 (5)	5.2 (1)
C4	0.7297 (4)	0.0399 (2)	0.3477 (5)	4.8 (1)
C5	0.8581 (4)	0.0180 (2)	0.3528 (5)	4.7 (1)
C6	0.9379 (4)	0.0504 (2)	0.2975 (4)	3.86 (9)
C7	1.1457 (3)	0.0991 (2)	0.1730 (4)	2.99 (8)
C8	1.2233 (4)	0.0992 (2)	0.3062 (5)	4.05 (9)
C9	1.3393 (4)	0.0593 (2)	0.3224 (5)	4.8 (1)
C10	1.3792 (4)	0.0199 (2)	0.2052 (6)	5.1 (1)
C11	1.3047 (4)	0.0207 (2)	0.0731 (5)	4.7 (1)
C12	1.1884 (4)	0.0600 (2)	0.0559 (4)	3.75 (9)
C13	0.9333 (3)	0.1486 (2)	−0.0309 (4)	3.03 (8)
C14	0.9526 (4)	0.1945 (2)	−0.1092 (4)	4.4 (1)
C15	0.9160 (5)	0.1934 (2)	−0.2594 (5)	5.6 (1)
C16	0.8573 (4)	0.1473 (2)	−0.3300 (4)	4.8 (1)
C17	0.8352 (4)	0.1017 (2)	−0.2540 (5)	4.6 (1)
C18	0.8735 (4)	0.1023 (2)	−0.1048 (4)	3.98 (9)
C19	0.8773 (3)	0.4075 (2)	0.2462 (4)	2.89 (8)
C20	0.8885 (4)	0.4692 (2)	0.2514 (4)	4.01 (9)
C21	0.7942 (4)	0.5103 (2)	0.1813 (5)	4.6 (1)
C22	0.6867 (4)	0.4914 (2)	0.1068 (5)	4.8 (1)
C23	0.6759 (4)	0.4311 (2)	0.0986 (5)	4.6 (1)
C24	0.7699 (4)	0.3891 (2)	0.1665 (4)	3.67 (9)
C25	1.1475 (3)	0.3813 (2)	0.3287 (4)	2.96 (8)
C26	1.1874 (4)	0.3873 (2)	0.1891 (4)	4.19 (9)
C27	1.2974 (4)	0.3988 (2)	0.1713 (5)	5.2 (1)
C28	1.3687 (4)	0.4229 (2)	0.2893 (5)	5.6 (1)
C29	1.3303 (4)	0.4266 (2)	0.4252 (5)	5.7 (1)
C30	1.2202 (4)	0.4053 (2)	0.4464 (4)	4.3 (1)
C31	0.9753 (3)	0.3691 (2)	0.5364 (4)	2.79 (7)
C32	0.8798 (4)	0.4145 (2)	0.5867 (4)	3.90 (9)
C33	0.8656 (4)	0.4234 (2)	0.7356 (4)	4.9 (1)
C34	0.9459 (4)	0.3883 (2)	0.8330 (4)	4.8 (1)
C35	1.0409 (4)	0.3435 (2)	0.7853 (4)	4.4 (1)
C36	1.0559 (4)	0.3326 (2)	0.6368 (4)	3.61 (9)
C37	0.5273 (4)	0.2161 (2)	−0.2073 (5)	5.0 (1)
C38	0.3287 (5)	0.1525 (2)	−0.2131 (7)	8.3 (2)
C39	0.5696 (5)	0.3280 (2)	−0.2805 (6)	6.6 (1)
C40	0.8429 (4)	0.2583 (2)	0.3291 (5)	4.16 (9)
C41	0.2909 (4)	0.2368 (2)	0.2232 (5)	4.7 (1)
C42	1.4277 (4)	0.2350 (2)	0.2297 (6)	7.3 (2)

[a] B values for anisotropically refined atoms are given in the form of the isotropic equivalent thermal parameter defined as $(4/3)[a^2B(1,1) + b^2B(2,2) + c^2B(3,3) + ab(\cos\gamma)B(1,2) + ac(\cos\beta)B(1,3) + bc(\cos\alpha)B(2,3)]$.

(33) Tsigdinos, G. A.; Hallada, C. J. *Inorg. Chem.* **1968**, *7*, 437.
(34) Siedle, A. R.; Filipovich, G.; Toren, P. G.; Palensky, F. J.; Cook, E.; Newmark, R. A.; Stebbings, W. E.; Melancon, K. *J. Organomet. Chem.* **1983**, *246*, 83.
(35) Penner-Hahn, J. E.; Elbe, K. S.; McMurray, T. J.; Renner, M.; Balch, A. L.; Groves, J. T.; Dawson, J. H.; Hodgson, K. O. *J. Am. Chem. Soc.* **1986**, *108*, 7816.

$[(Ph_3P)_2Rh(CO)]_4SiW_{12}O_{40}$ (6). Method A. A 1.65-g sample of **2** was placed in a flask and connected to a high-vacuum line via a liquid-N_2 trap. After evacuation to base pressure (ca. 3×10^{-6} mm), the compound was heated under dynamic vacuum for 22 h with a 150 °C oil bath. Upon cooling, 1.55 g of product remained in the flask.

Method B. To a solution of 1.3 g of **1** in 30 mL of warm, deoxygenated ethanol was added with vigorous stirring and strict exclusion of air a solution of 0.82 g of hydrated $(H_3O)_4SiW_{12}O_{40}$. The product, which precipitated from the reaction mixture, was collected on a Schlenk filter, washed with ethanol, and then dried under high vacuum. The yield was 1.2 g.

Compound **11** was similarly prepared by using the deep blue solution of $PMo_{12}O_{40}^{4-}$ obtained by addition of 1.1 mL of a deoxygenated 0.2 M solution of $NaBH_4$ in ethanol to 0.38 g of hydrated $(H_3O)_3PMo_{12}O_{40}$.

Resolvation of $[(Ph_3P)_2Rh(CO)]_4SiW_{12}O_{40}$. Acetonitrile, 8 mL, was added by vacuum transfer to 0.72 g of **6**, which was then heated at 105 °C for 16 h in a sealed tube. Filtration afforded 0.69 g of **1**, identified by elemental and IR analyses.

Isomerization of 1-Hexene. In a glass tube were placed 0.03 g of **6**, 2 mL of toluene, 0.6 mL of 1-hexene, and a magnetic strirrer bar. The mixture was degassed by two freeze–pump–thaw cycles, brought to atmospheric pressure with argon, and then stirred and heated at 100 °C for 12 h. After cooling to room temperature, the insoluble catalyst, unchanged by IR analysis, was removed by filtration. The olefin mixture was analyzed by ^{13}C NMR spectroscopy. This method, preferred on account of its rapidity, employs a Varian XL-200 instrument. $Cr(acac)_3$, 0.02 M, was added to the samples to reduce the relaxation time, and nOe-suppressed spectra were obtained with a 5.0-s recycle time and 16-μs (90°) pulses. Quantitative ratios of hydrocarbons were obtained by integration of the aliphatic methylene resonances only so as to minimize systematic errors arising from different relaxation times and nuclear Overhauser factors. Chemical shifts for hexene isomers were taken from the literature.[36-38]

Hydroformylation of 1-Hexene. A mixture of 1 mL of the olefin, 10 mL of toluene, and 0.1 g of **6** was placed in a glass-lined autoclave (use of a glass liner, which is easily cleaned, obviates contamination of the steel autoclave with any catalyst from a previous run). This was evacuated and back-filled to 1000 psi with 1:1 H_2–CO and then heated at 100 °C for 3 h. After cooling to room temperature, the gas phase was vented and the liquid phase filtered through a fine-porosity glass frit to remove any entrained catalyst. The aldehyde mixture was then analyzed by GC.

Aldehyde Oxidation. A hydroformylation reaction was carried out as described above. After removal of an aliquot for analysis, the autoclave was twice evacuated and back-filled to 650 psi with air. Heating at 100 °C was carried out for 4 h, after which the autoclave was cooled to room temperature and the contents removed for analysis.

Reaction of NO and CO. A 0.035-g sample of **6** was placed in a $4 \times {}^1/_4$ in. glass tube fitted with a vacuum stopcock. The vessel was evacuated and back-filled to 160-mm pressure with a 1:1 mixture of CO and NO. After standing for 3 days with occasional shaking, the gas phase was analyzed by GC–MS. This revealed that 12% of the CO had been converted to CO_2; only trace amounts of N_2O were detected.

X-ray Structure Determination. A summary of crystal and intensity data for $[(Ph_3P)_2Rh(CO)(CH_3CN)][HC(SO_2CF_3)_2]$ is presented in Table VII. Table VIII lists positional parameters and their estimated standard deviations. The crystal class and space group were determined by the Enraf-Nonius CAD4-SDP-PLUS peak search, centering, and indexing programs,[39] by the presence of systematic absences observed during data collection, and by successful solution and refinement. The intensities of three standard reflections were measured every 60 min; a decrease in intensity of 14.9% was observed. A linear correction from 1.000 to 1.085, with an average value of 1.041, on I was applied with use of program DECAY.[39] Empirical absorption correction was applied by use of ψ-scan data and programs PSI and EAC.[39]

The structure was solved by conventional heavy-atom techniques. The Rh atom was located by Patterson synthesis, and full-matrix least-squares refinement and difference Fourier calculations were used to locate all remaining non-hydrogen atoms. The atomic scattering factors were taken from the usual tabulation,[40] and the effects of anomalous dispersion were included in F_c by using the Cromer and Ibers values of $\Delta f'$ and $\Delta f''$.[41] Hydrogen atom positions were calculated for the Ph_3P and $HC(SO_2CF_3)_2^-$ groups but were not refined. The final difference Fourier map did not reveal any chemically significant peaks. The largest peak observed was 0.34 e Å^{-3}. The final positional and thermal parameters of the refined and calculated atoms are provided as supplementary material.

Acknowledgment. We are grateful to members of the 3M Analytical and Properties Research Laboratory for spectroscopic and analytical data, to W. T. Conway for the thermal analysis data, to C. Brozek and J. Schroepfer for the TPD spectra, and to Manfred Riechert, 3M Process Technologies Laboratory, for carrying out the high-pressure reactions. X-ray absorption data were recorded at the Stanford Synchrotron Radiation Laboratory, which is supported by the U.S. Department of Energy and the Research Resources Division of the National Institutes of Health. We are most grateful to Prof. W. G. Klemperer for helpful discussions and a sample of $(Bu_4N)_2[(Me_5C_5Rh)W_5O_{18}(TiC_5H_5)]$ and to Prof. V. W. Day for the results of the X-ray crystal structure determination in advance of publication.

Supplementary Material Available: A summary of crystallographic procedures, tables of crystallographic parameters, calculated hydrogen atom positions (Table S1), bond distances and angles (Table S2), and torsion angles and least-squares planes (Table S3), and ORTEP diagrams (22 pages); a listing of observed and calculated structure factors (Table S4) (47 pages). Ordering information is given on any current masthead page.

(36) Grant, D. M.; Paul, E. G. *J. Am. Chem. Soc.* **1964**, *86*, 2984.
(37) De Haan, J. W.; Van de Ven, L. J. M. *Org. Magn. Reson.* **1973**, *5*, 147.
(38) Sadtler Research Laboratories, Philadelphia, PA, spectrum S3946C.
(39) All calculations were carried out on PDP 8A and 11/34 computers with use of the Enraf-Nonius CAD-4 SDP-PLUS programs. This crystallographic computing package is described by: Frenz, B. A. In *Computing in Crystallography*; Schenk, H., Olthof-Hazekamp, R., van Konigsveld, H., Bassi, G. C., Eds.; Delft University: Delft, Holland, 1978; pp 64–71. Frenz, B. A. In *Structure Determination Package and SDP-PLUS User's Guide*; B. A. Frenz and Associates: College Station, TX, 1982.
(40) Cromer, D. T.; Waber, J. T. *International Tables for X-Ray Crystallography*; Kynoch Press: Birmingham, England, 1974; Vol. IV, Tables 2.2.4 and 2.3.1.
(41) Cromer, D. T.; Ibers, J. A. In ref 40.